© 2014. Published by The Company of Biologists Ltd | Journal of Cell Science (2014) 127, 137–146 doi:10.1242/jcs.133553

RESEARCH ARTICLE

14-3-3θ facilitates plasma membrane delivery and function of mechanosensitive connexin 43 hemichannels

Nidhi Batra*, Manuel A. Riquelme*, Sirisha Burra and Jean X. Jiang‡

ABSTRACT

Intracellular signaling in osteocytes activated by mechanical loading is important for bone formation and remodeling. These signaling events are mediated by small modulators released from Cx43 hemichannels (HC). We have recently shown that integrin α5 senses the mechanical stimulation and induces the opening of Cx43 HC; however, the underlying mechanism is unknown. Here, we show that both Cx43 and integrin α5 interact with 14-3-3θ, and this interaction is required for the opening of Cx43 HC upon mechanical stress. The absence of 14-3-3θ prevented the interaction between Cx43 and integrin α5, and blocked HC opening. Furthermore, it decreased the transport of Cx43 and integrin α5 from the Golgi apparatus to the plasma membrane. Mechanical loading promoted the movement of Cx43 to the surface which was associated not only with an increase in 14-3-3θ levels but also its interaction with Cx43 and integrin α5. This stimulatory effect on forward transport by mechanical loading was attenuated in the absence of 14-3-3θ and the majority of the Cx43 accumulated in the Golgi. Disruption of the Golgi by brefeldin A reduced the association of Cx43 and integrin α5 with 14-3-3θ, further suggesting that the interaction is likely to occur in the Golgi. Together, these results define a previously unidentified, scaffolding role of 14-3-3θ in assisting the delivery of Cx43 and integrin α5 to the plasma membrane for the formation of mechanosensitive HC in osteocytes.

KEY WORDS: 14-3-3, Connexion, Hemichannel

INTRODUCTION

Bone tissue orchestrates the remodeling process of bone turnover in coordination with the three types of bone cells, osteoblasts, osteocytes and osteoclasts. During this process, the bone is subjected to mechanical forces from its surrounding environment. Several important biochemical signals are generated through the mechanical forces that regulate bone cell behavior. Previous studies suggest that fluid flow over the network of osteocytes embedded within the bone is the main signal-generating factor and that osteocytes are the major cell types involved in producing the response (Hughes-Fulford, 2004; Jacobs et al., 2010). As a matter of fact, these cells are capable of sensing physical alterations in bone primarily owing to the presence of molecules whose location and sensitivity to mechanical signals allows them to detect the changes. One of those molecules is connexin (Cx) 43, which is abundant in the bone osteocytes and is responsible for the formation of gap junctions and hemichannels (HC) in these cells (Batra et al., 2012b; Civitelli, 2008). Gap junctions are the only channels mediating direct communication between two adjacent cells. These channels are formed from the docking of two HC (connexons). HC are formed when six connexins join to form a connexon on the cell surface. HC mainly maintain communication and exchange of small molecules between the cell and its external environment (Goodenough and Paul, 2003). Both gap junctions and HC allow the passage of molecules less than 1 kDa. Unlike the majority of the other membrane proteins, Cx43 is reported to be assembled into hexameric connexons in the trans-Golgi network (Musil and Goodenough, 1993). We showed previously that fluid flow shear stress (FFSS) promotes the opening of Cx43 HC in primary osteocytes and osteocytic MLO-Y4 cells, leading to the release of anabolic factors such as prostaglandins (Cherian et al., 2005). Another study reported that FFSS opens Cx43 HC on the plasma membrane in osteocytes to trigger the release of ATP by a protein-kinase-C-mediated pathway (Genetos et al., 2007). Given that mechanical forces are also known to deform the extracellular matrix, they can alter the integrin protein conformation leading to activation of secondary messenger pathways or exert their effect directly on the cell surface protein–integrin complex (Silver and Siperko, 2003). We have previously shown that FFSS increases the assembly and cell surface expression of Cx43 HC (Siller-Jackson et al., 2008). We recently demonstrated that integrin α5 interacts with Cx43 in osteocytic cells and this interaction, in conjunction with the activation of integrin α5, is required for the opening of Cx43 HC in response to mechanical loading (Batra et al., 2012a).

The major question is how does Cx43 co-assemble with integrin α5 on the plasma membrane to form the mechano-sensitive HC complex. By investigating the possible binding partners of Cx43 and integrin α5 that could serve as a scaffolding protein for these two proteins, 14-3-3θ emerged as a potential candidate. Cx43 is the only connexin that contains a consensus 14-3-3 mode I binding sequence motif at the cytoplasmic C-terminus and it can directly interact with 14-3-3θ (Park et al., 2006). In addition, our database analysis showed that integrin α5 also contains a 14-3-3 binding motif in the cytoplasmic domain. 14-3-3 proteins exist as either homo- or heterodimers with a molecular mass of 30 kDa (Liu et al., 1995; Xiao et al., 1995). It is an evolutionarily conserved family of proteins, which possesses seven different mammalian isoforms with three conserved binding motifs – mode I, mode II and a relatively new mode III (Muslin et al., 1996; Shikano et al., 2005; Yaffe et al., 1997). Interaction of 14-3-3 with its target protein requires binding of the dimer to the two binding sites either on the same protein or on separate proteins (Gardino et al., 2006; Liu et al., 1995; Xiao et al., 1995). This unique protein can perform any of the following three tasks on the target protein upon interaction: stabilizing certain conformations (clamping) (Yaffe, 2002), hiding or sorting structural motifs (masking) for

Department of Biochemistry, University of Texas Health Science Center, San Antonio, TX 78229-3900, USA.
*These authors contributed equally to the work

‡Author for correspondence (jiangj@uthscsa.edu)

Received 19 April 2013; Accepted 6 October 2013

Journal of Cell Science

Journal of Cell Science (2014) 127, 137–146 doi:10.1242/jcs.133553

intracellular transport of targeted proteins to the plasma membrane (Nufer and Hauri, 2003; O'Kelly et al., 2002; Yuan et al., 2003) or facilitating the interaction of the target protein with other proteins by providing a platform for the protein recruitment at specific cellular locations (scaffolding) (Mrowiec and Schwappach, 2006). None of these tasks is sufficiently well understood in membrane proteins that interact with 14-3-3, nor is the scaffolding action of 14-3-3 in the regulation of membrane protein trafficking or assembly. Our study suggests a scaffolding action of 14-3-3θ that binds to Cx43 and integrin α5, and assists these two proteins to migrate from the Golgi apparatus to the plasma membrane. Assembly of Cx43 on the plasma membrane is essential for the opening of HC to mediate the anabolic function of osteocytes in response to mechanical loading.

RESULTS

14-3-3θ interacts with Cx43 and integrin α5, and is required for the interaction between integrin α5 and Cx43

Recently, we demonstrated that the association between Cx43 and integrin α5 played a crucial role for the opening of Cx43 HC in response to FFSS, a process important for the release of anabolic factors (Batra et al., 2012a). A previous *in vitro* study by Park et al. showed that Cx43 can directly bind to 14-3-3θ (Park et al., 2006). We found that integrin α5 also contains a consensus 14-3-3θ binding site. Immunoprecipitation experiment using Cx43 antibody showed that Cx43 could co-immunoprecipitate 14-3-3θ from lysates of osteocytic MLO-Y4 cells (Fig. 1A). Conversely, Cx43 was present in the co-immunoprecipitates using anti-14-3-3θ antibody (Fig. 1B). These results suggest that Cx43 interacts with 14-3-3θ. The interaction between integrin α5 and 14-3-3θ was also demonstrated. 14-3-3θ was detected in the immunoprecipitates of MLO-Y4 lysates using anti-integrin α5 antibody (Fig. 1C). The direct binding assay using a peptide containing integrin α5 C-terminus to pull down purified His-tagged 14-3-3θ confirmed the specific interaction between 14-3-3θ and integrin α5 (Fig. 1D).

To determine the importance of 14-3-3θ in the interaction between Cx43 and integrin α5, we reduced the expression of 14-3-3θ using specific siRNA (Fig. 2A). Approximately 80% of 14-3-3θ expression was abolished with 30 nM 14-3-3θ siRNA and further reduction occurred with 60 and 75 nM (Fig. 2A, lower panel). The treatment with 14-3-3θ siRNA had no effect on the expression levels of Cx43 (Fig. 2A, right upper panel) or integrin α5 (Fig. 2, right lower panel). Co-immunoprecipitation studies using integrin α5 antibody showed that only in the cells treated with 14-3-3θ siRNA was the interaction between Cx43 and integrin α5 disrupted (Fig. 2B). These results indicate that 14-3-3θ may function as a scaffold in facilitating the interaction between Cx43 and integrin α5.

FFSS-mediated HC opening is blocked and the cell surface expression of Cx43 is reduced in the absence of 14-3-3θ

Association between Cx43 and integrin α5 is required for the opening of Cx43 HC in osteocytes (Batra et al., 2012a). To determine the influence of 14-3-3θ on HC function, cells treated

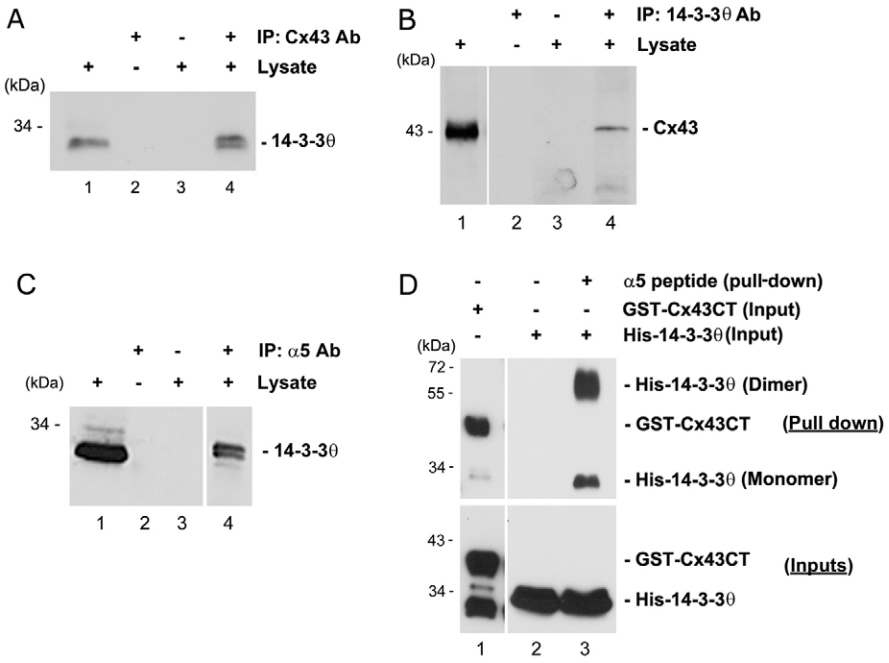

Fig. 1. 14-3-3θ interacts with Cx43 and integrin α5. (A) Lysates of MLO-Y4 cells were immunoprecipitated with anti-Cx43 antibody (lane 4). Cell lysates (lane 1) and immunoprecipitates (lanes 2–4) were immunoblotted with anti-14-3-3θ antibody. Beads incubated only with either 14-3-3θ antibody (lane 2) or lysates (lane 3) served as negative controls. (B) Cell lysates were immunoprecipitated with anti-14-3-3θ antibody (lane 4), and cell lysates (lane 1) and immunoprecipitates (lanes 2–4) were immunoblotted with anti-Cx43 antibody. Beads incubated only with either 14-3-3θ antibody (lane 2) or lysates (lane 3) served as negative controls. (C) Cell lysates were immunoprecipitated with anti-integrin α5 antibody (lane 4), and cell lysates (lane 1) and immunoprecipitates (lanes 2–4) were immunoblotted with anti-14-3-3θ antibody. Beads incubated only with integrin α5 antibody (lane 2) or lysates (lane 3) served as negative controls. (D) Purified GST–Cx43CT (lane 1) or His–14-3-3θ (lanes 2 and 3) was pulled down using a peptide containing the C-terminus of integrin α5 (α5 peptide) conjugated with magnetic beads. Pull down of His–14-3-3θ with magnetic beads alone served as negative control (lane 2). Elutes (upper panel) from the pull-down assay were immunoblotted with either anti-Cx43 antibody (lane 1) or anti-14-3-3θ antibody (lane 2 and 3). The inputs (lower panel) were immunoblotted with either GST (lane 1) or 14-3-3θ (lanes 2 and 3) antibody.

Journal of Cell Science (2014) 127, 137–146 doi:10.1242/jcs.133553

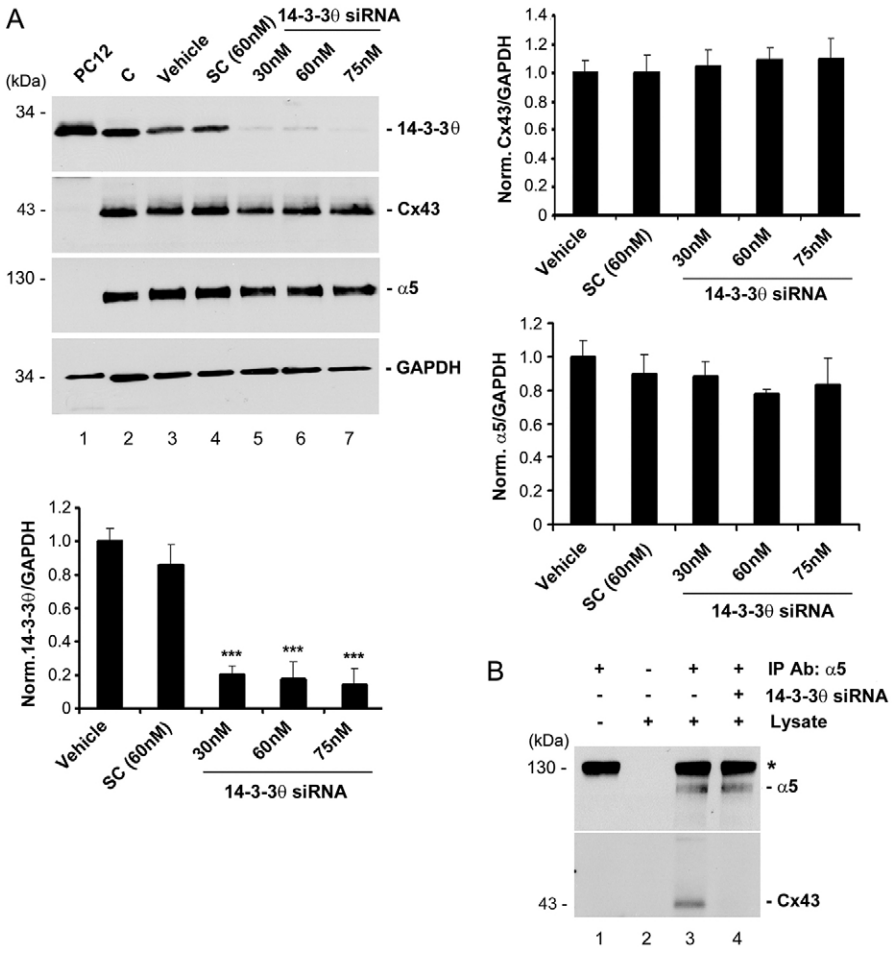

Fig. 2. 14-3-3θ is required for the interaction between Cx43 and integrin α5. (A) Knockdown of 14-3-3θ expression by a siRNA. MLO-Y4 cells were treated with 14-3-3θ siRNA (lanes 5–7), siRNA from a scrambled sequence (SC; lane 4), only the transfection reagent (Vehicle; lane 3) or were left untreated as the control (C) (lane 2). Lysates of PC12 cells, known to have high 14-3-3θ expression (lane 1) or MLO-Y4 cells were immunoblotted with anti-14-3-3θ, Cx43, integrin α5 or GAPDH antibody. The ratio of the band intensity of 14-3-3θ (left lower panel), Cx43 (right upper panel) or integrin α5 (right lower panel) to GAPDH was quantified. $n=3$. ***$P<0.001$ for 14-3-3θ siRNA versus vehicle and SC (left lower panel). (B) Knockdown of 14-3-3θ disrupted the association between Cx43 and integrin α5. Lysates of MLO-Y4 cells transfected with 14-3-3θ siRNA (lanes 3 and 4) was immunoprecipitated with anti-integrin α5 antibody. Eluates from beads were immunoblotted with anti-integrin α5 or Cx43 antibody. Beads incubated only with integrin α5 antibody (lane 1) or lysates (lane 2) served as negative controls.

with 14-3-3θ siRNA, scrambled siRNA and vehicle control were subjected to FFSS, and HC opening was monitored by Lucifer Yellow (LY; molecular mass 457 Da) dye uptake. The opening of HC, as indicated by LY dye uptake, in response to FFSS was observed in cells treated with scrambled siRNA or vehicle controls, but a reduction of HC activity was observed in cells treated with 14-3-3θ siRNA (Fig. 3A). The quantification results further confirmed this observation (Fig. 3B), thereby suggesting a role of 14-3-3θ in HC activity (Fig. 3).

14-3-3θ, as a scaffolding protein, has been shown to maintain protein stability and assist intracellular trafficking of proteins (Mrowiec and Schwappach, 2006). Given that knockdown of 14-3-3θ expression had no effect on levels of total Cx43 and integrin α5 proteins, the depletion of 14-3-3θ may have an effect on the

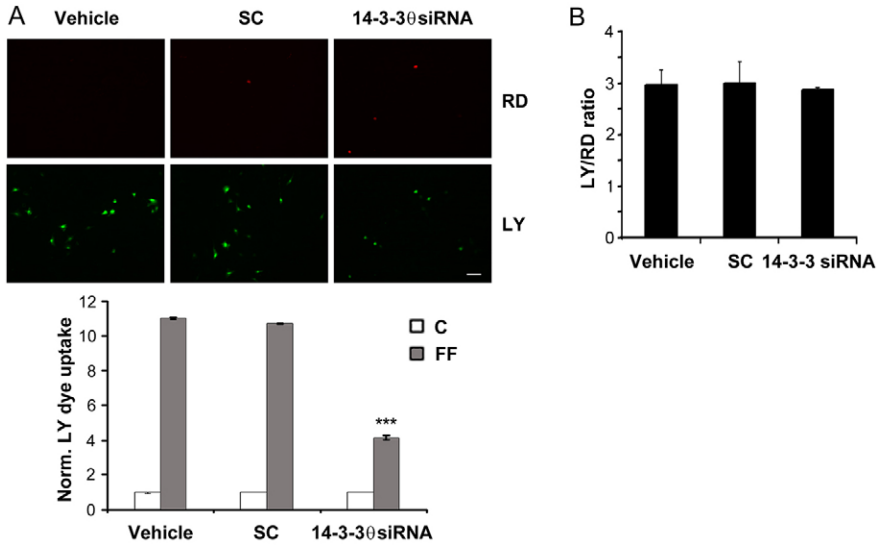

Fig. 3. Knockdown of 14-3-3θ inhibits HC opening induced by FFSS, but not gap junctional coupling. (A) 14-3-3θ knockdown inhibits FFSS-induced HC opening. MLO-Y4 cells treated with transfection reagent (vehicle), scrambled siRNA (SC) or 14-3-3θ siRNA (30 nM) were subjected to static (C) or 16 dynes/cm^2 of FFSS (FF) for 2 hours and LY dye uptake was assayed. Rhodamine dextran (RD; 10 kDa) uptake was used as a control for detection of membrane integrity. Fluorescence images were taken of cells subjected to FFSS (upper panel) and the level of LY dye uptake was quantified (lower panel). Scale bar: 50 μm. ***$P<0.001$ for 14-3-3θ-siRNA-treated versus vehicle and SC; $n=3$. (B) 14-3-3θ knockdown had no effect on the gap junction coupling. A scrape-loading LY dye transfer experiment was performed on MLO-Y4 cells treated with 14-3-3θ siRNA, SC or vehicle and the degree of dye transfer was quantified as the ratio of cells receiving LY to RD. $n=3$.

Journal of Cell Science (2014) 127, 137–146 doi:10.1242/jcs.133553

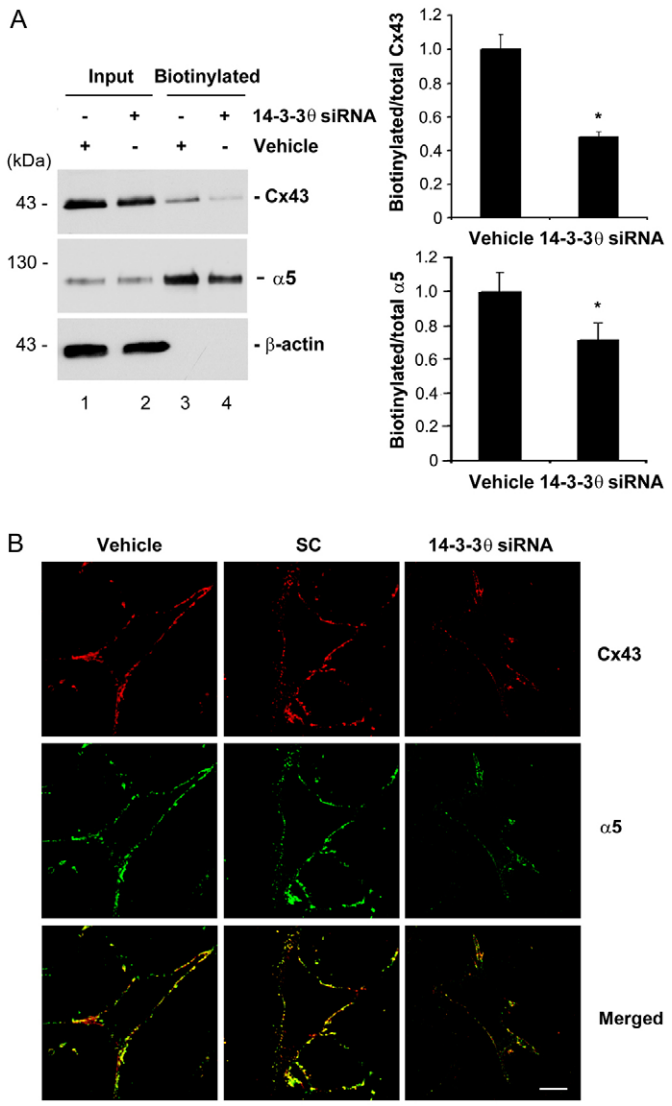

Fig. 4. 14-3-3θ is involved in the cell surface expression of Cx43 and integrin α5. (A) 14-3-3θ knockdown reduces the cell surface expression of Cx43 and integrin α5 as detected by cell surface biotinylation. MLO-Y4 cells were treated with 30 nM 14-3-3θ siRNA or vehicle control. Surface expression of Cx43 and integrin α5 was determined by a surface biotinylation assay. Cell lysates prior to loading on avidin-conjugated beads (input, lanes 1 and 2) and bound to avidin beads (biotinylated, lanes 3 and 4) were immunoblotted with anti-Cx43, integrin α5 or β-actin antibody. The relative ratio of biotinylated to total (Input) Cx43 or integrin α5 was quantified using densitometric measurements of the band intensity (right, upper and lower panel, respectively). *$P<0.05$ for 14-3-3θ-siRNA-treated versus vehicle control; $n=3$. (B) 14-3-3θ knockdown reduces the cell surface expression of Cx43 and integrin α5 as detected by immunofluorescence. Cell surface labeling of Cx43 and integrin α5 from non-detergent permeable cells treated with 14-3-3θ siRNA, scrambled siRNA (SC) or transfection reagent (vehicle) were detected by dual-immunofluorescence staining with anti-Cx43 and integrin α5 antibodies followed by Rhodamine-labeled anti-rabbit IgG or FITC-labeled anti-sheep IgG, respectively. Scale bar: 10 μm.

surface expression of Cx43 and integrin α5, leading to reduced formation of HC on the surface. A cell surface biotinylation assay showed that the level of biotinylated Cx43 (Fig. 4A, right upper panel) or integrin α5 (Fig. 4A, right lower panel) was significantly ($P<0.05$) reduced. Immunofluorescence staining of non-detergent permeable cells showed that the surface presence of both Cx43 and integrin α5 was decreased compared with that of cells treated with vehicle or scrambled siRNA (SC; Fig. 4B). Merged images further showed the colocalization of Cx43 and integrin α5 on the cell surface and the signals for both proteins decreased with the knockdown of 14-3-3θ. Hence, our results suggest that although 14-3-3θ has minimal effect on total protein levels of Cx43 and integrin α5, it is required for cell surface expression of both proteins.

14-3-3θ is crucial for the delivery of Cx43 from the Golgi to the cell surface in response to FFSS

Cx43 is reported to be localized in the Golgi where it oligomerizes from monomers to hexamers (Musil and Goodenough, 1993), and then moves to the surface to form HC. Dual immunostaining with anti-Cx43 and Golgi 58K marker protein showed that in cells treated with 14-3-3θ siRNA, more Cx43 accumulated in the Golgi and less on the cell surface than when cells were treated with vehicle control, as indicated by perinuclear staining and co-localization with the 58K Golgi marker protein (Fig. 5, upper panel). Quantification of co-localization using Pearson's correlation coefficient (Rr-value) further confirmed the significant ($P<0.05$) increase of Cx43 accumulated in the Golgi (Fig. 5, lower panel). This data suggests that 14-3-3θ is required for movement of Cx43 from Golgi to the cell surface.

In our previous published study, we showed that the surface expression of Cx43 increases after 2 hours of FFSS (Siller-Jackson et al., 2008). Co-immunostaining of Cx43 and Golgi 58K protein in the absence and presence of FFSS were performed (Fig. 6A). In contrast to the majority of Cx43, which colocalized with 58K protein in the absence of FFSS, the extent of the perinuclear staining of Cx43 was considerably reduced in the presence of FFSS as indicated by a significant (**$P<0.01$)

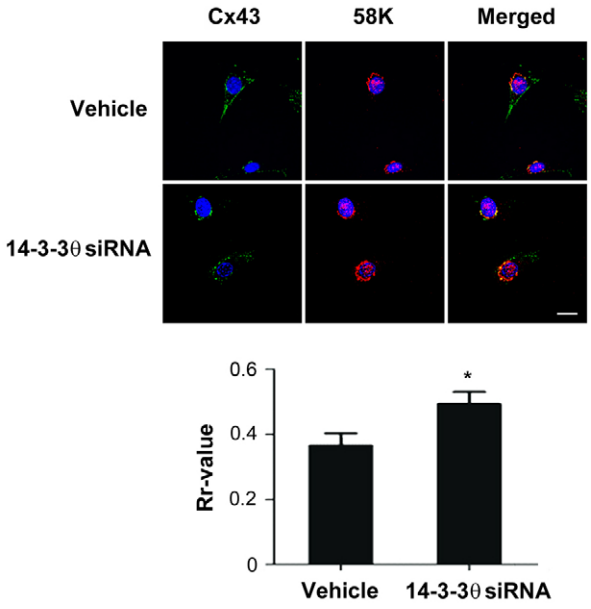

Fig. 5. 14-3-3θ is involved in the exit of Cx43 from the Golgi. MLO-Y4 cells treated with 14-3-3θ siRNA or transfection reagent (vehicle) were dual-immunostained with anti-Cx43 and 58K Golgi marker antibodies, followed by FITC and Rhodamine-conjugated secondary antibodies, respectively. The nuclei were stained with DAPI. The colocalization is shown in the merged images. Scale bar: 10 μm. The degree of colocalization was quantified using the Pearson's correlation coefficient (Rr) from the ImageJ software (lower panel). *$P<0.05$ for 14-3-3θ-siRNA-treated versus vehicle control; $n=3$.

Journal of Cell Science (2014) 127, 137–146 doi:10.1242/jcs.133553

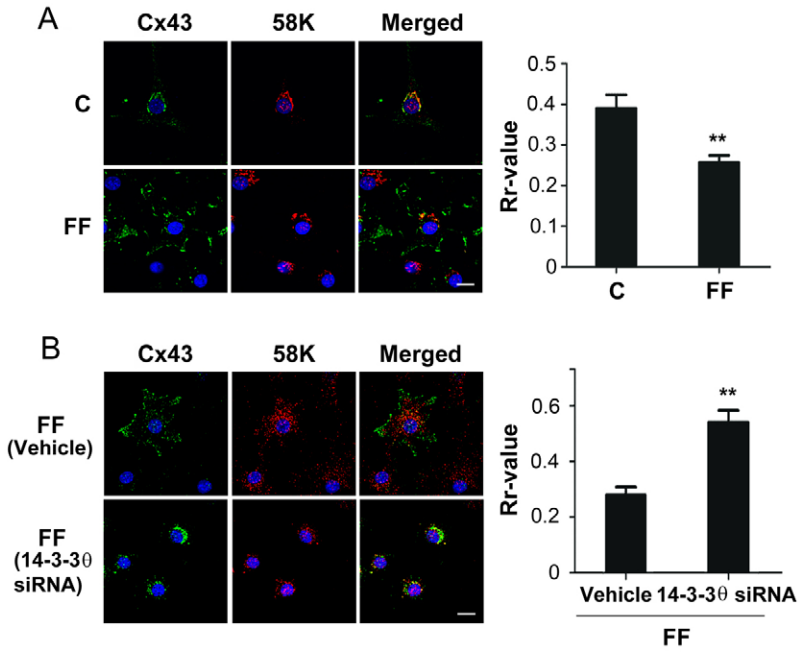

Fig. 6. Loss of 14-3-3θ attenuates the effect of FFSS on promoting the exit of Cx43 from the Golgi. (A) FFSS increases the exit of Cx43 from Golgi. MLO-Y4 cells subjected to FFSS (FF; 16 dynes/cm^2) for 2 hours were fixed and dual-immunostained with antibodies against Cx43 and 58K Golgi marker protein. The colocalization is shown in the merged images. The overlap of fluorescence signals were calculated using ImageJ software and a correlation coefficient (Rr) value was obtained that describes the extent of overlap of the two colors. Scale bar: 10 μm. $^{**}P<0.01$ for FF versus control; $n=3$. (B) 14-3-3θ knockdown blocks the increased Golgi exit of Cx43 induced by FFSS. MLO-Y4 cells treated with 30 nM 14-3-3θ siRNA or transfection reagent (vehicle) were subjected to FFSS (16 dynes/cm^2) for 2 hours and fixed cells were dual-immunostained with antibodies against Cx43 and 58K Golgi marker protein. The colocalization is shown in the merged images. The overlap of fluorescence signals was calculated using ImageJ software and a correlation coefficient (Rr) value was obtained. Scale bar: 10 μm. $^{**}P<0.01$ for FF, vehicle versus 14-3-3θ siRNA treatment; $n=3$.

decrease in its colocalization with 58K protein (Fig. 6A, right panel). These results suggest that FFSS promotes the exit of Cx43 from Golgi leading to the forward transport of Cx43 to the cell surface. However, absence of 14-3-3θ attenuated the FFSS-promoted forward transport of Cx43 as observed by a significant ($^{**}P<0.01$) increase in the colocalization of Cx43 perinuclear staining and Golgi 58K (Fig. 6B).

Cx43 is reported to be assembled in the trans-Golgi network (TGN) to form hexameric connexons (Musil and Goodenough, 1993). We therefore assessed whether Cx43, integrin α5 and 14-3-3θ are located in the TGN by co-immunolabeling with an antibody against a TGN marker, TGN38 (supplementary material Fig. S1). We observed minimal colocalization of Cx43, integrin α5 and 14-3-3θ with TGN38, indicating that Cx43 assembly and its association with 14-3-3θ and integrin α may not occur in TGN in osteocytes.

FFSS enhanced 14-3-3θ expression, and the interaction of 14-3-3θ with Cx43 and integrin α5

We then examined whether the level of 14-3-3θ is enhanced by FFSS, in correlation with the increased surface expression of Cx43. The protein level of 14-3-3θ increased after 30 minutes of FFSS and even more after 2 hours, but declined after 24 hours of FFSS (Fig. 7A). The level of 14-3-3θ is correlated with the closure of HC after 24 hours of FFSS as we observed previously (Siller-Jackson et al., 2008). Correspondingly, the interaction between 14-3-3θ and Cx43 was substantially increased by 2.5-fold in MLO-Y4 cells subjected to FFSS (Fig. 7B). A similar increase in the interaction between 14-3-3θ and integrin α5 upon FFSS was observed (Fig. 7C). These results indicated that FFSS enhanced the interaction between 14-3-3θ and Cx43/integrin α5, possibly as a result of elevated 14-3-3θ levels, which led to the delivery of more Cx43 and integrin α5 proteins from the Golgi to the plasma membrane to form more functional HC.

The Golgi is a major site for the association of Cx43 and integrin α5 with 14-3-3θ

As shown above, depletion of 14-3-3θ results in the accumulation of Cx43 and integrin α5 in the Golgi. To determine whether the association with 14-3-3θ occurs in the Golgi, we treated the cells with brefeldin A (BFA), a commonly used inhibitor that interferes with the transport from the ER to the Golgi apparatus leading to the collapse of the Golgi stacks. The treatment with BFA caused the intracellular accumulation of Cx43, and co-localization with 14-3-3θ was significantly ($^{*}P<0.05$) decreased under both static (Fig. 8A) and fluid flow (Fig. 8B) conditions. The quantification data are presented in the right panels of the corresponding images. Upon BFA treatment, the colocalization between Cx43 and integrin α5 was also significantly ($^{**}P<0.01$) reduced under both static and FFSS conditions (Fig. 8C,D). Note that the fluorescence signals in BFA-treated cells appear to be weaker. However, immunoblotting result showed that BFA treatment increased the total Cx43 protein, but such an increase was not observed with 14-3-3θ and the β-actin control (Fig. 8E). These differences between total protein level and fluorescence signals could be caused by the oligomeric state of the proteins expressed in the cell. Together, these results suggest that the association of Cx43, integrin α5 and 14-3-3 is likely to occur in the Golgi apparatus.

DISCUSSION

Developmental, physiological and pathological processes rely on the biochemical signals activated upon the conversion of mechanical forces through a process called mechanotransduction (Orr et al., 2006). Application of force to the bone results in the flow of fluid that surrounds the osteocytic canalicular network, which has the capacity to alter the conformations of macromolecules and activate mechanosensitive channels (Batra et al., 2012b; Fritton and Weinbaum, 2009; Jacobs et al., 2010). We recently showed that FFSS induced the conformational activation of integrin α5β1 and its interaction with Cx43 resulting in the opening of Cx43 HC (Batra et al., 2012a). The opening of HC mediates the release of small factors including prostaglandins, important for anabolic function of the bone (Cherian et al., 2005). In this study, as illustrated in Fig. 9, we show that under static conditions, 14-3-3θ is required for the interaction between Cx43 and integrin α5, and mediates the

Journal of Cell Science (2014) 127, 137–146 doi:10.1242/jcs.133553

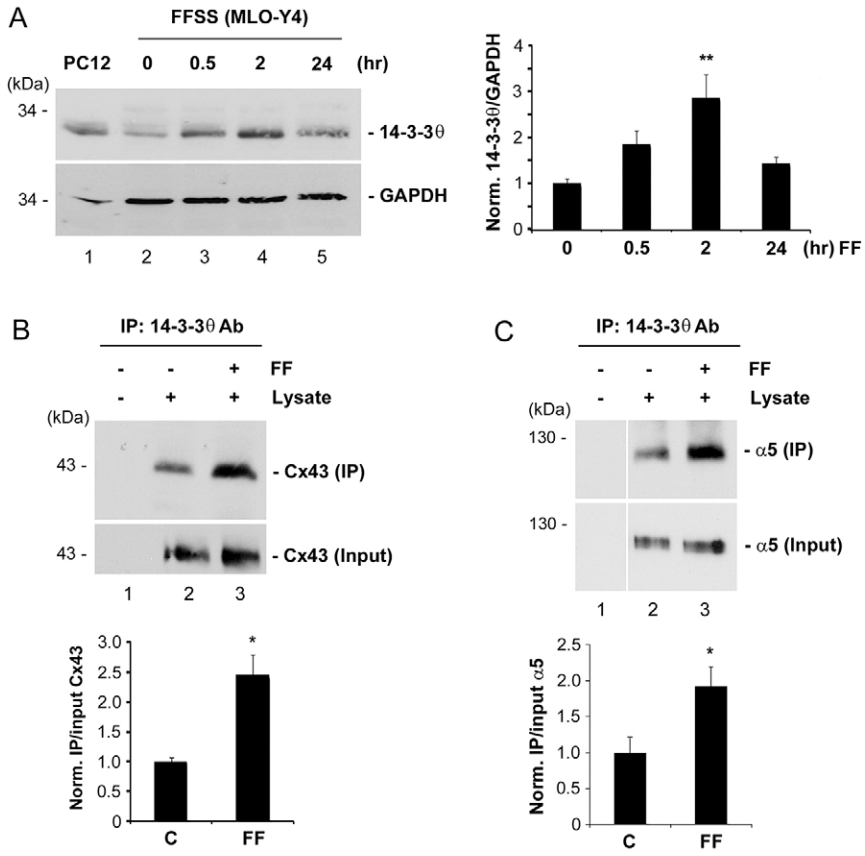

Fig. 7. FFSS increases 14-3-3θ expression and its interaction with Cx43 and integrin α5. (A) PC12 cell lysates (lane 1) or lysates of MLO-Y4 cells subjected to fluid flow for 0 (lane 2), 0.5 (lane 3), 2 (lane 4), and 24 (lane 5) hours were immunoblotted with anti-14-3-3θ or GAPDH antibody. Band intensity was quantified and the normalized ratio of 14-3-3θ to GAPDH was calculated (right panel). $^{**}P<0.01$ for 2 hours versus 0 hours; $n=3$. (B,C) Lysates of MLO-Y4 cells subjected to FFSS for 2 hours (lane 3) or non-fluid flow (lanes 1 and 2) were immunoprecipitated with anti-14-3-3θ antibody. Preloaded lysates (input) or eluates from beads were immunoblotted with anti-Cx43 (B) or anti-integrin α5 (C) antibody. Band intensity of Cx43 was quantified and the normalized ratio of eluates from beads (IP) to preloaded (input) was calculated (lower panel). In B,C, $^{*}P<0.05$ for FF versus non-FF (C); $n=3$.

forward transport of Cx43 from the Golgi to the cell surface. FFSS increases the level of 14-3-3θ and its association with Cx43 and integrin α5. Consequently, more Cx43 and integrin α5 molecules are delivered to the cell surface to accommodate the formation of functional HC in response to FFSS.

The interaction of Cx43 with other proteins is gaining considerable importance for their role in the regulation of Cx43 trafficking, assembly and disassembly as well as the dynamic modulation of channel opening (Chanson et al., 2007; Hervé et al., 2007). Although, 14-3-3 has been shown to interact with several integrins including β1, αLβ2 and α4 (Deakin et al., 2009; Han et al., 2001; Nurmi et al., 2006), our study is the first to show that 14-3-3θ interacts with integrin α5. More importantly, we show that 14-3-3θ is necessary for the interaction between Cx43 and integrin α5 because reduction of 14-3-3θ by siRNA impairs the association between these two proteins. Our recent study showed a weak, direct interaction between the C-terminus of Cx43 and integrin α5 (Batra et al., 2012a). This interaction is likely to be facilitated through the scaffolding action of 14-3-3θ by binding with both Cx43 and integrin α5 in order to bring these two proteins to physical proximity for interaction. Recently, we demonstrated that disrupting the binding between Cx43 and integrin α5 blocked Cx43 HC opening in these cells (Batra et al., 2012a). Consistently, we further observed that absence of 14-3-3θ not only abolished the interaction between Cx43 and integrin α5 but also blocked the HC opening in response to FFSS. 14-3-3θ serves as a scaffolding/chaperone protein and mediates the association and co-migration of Cx43 and integrin α5 to the plasma membrane for the formation and correct functioning of HC.

Knockdown of 14-3-3θ expression reduced the surface Cx43 levels by more than a half, but intriguingly, a lesser reduction was observed for integrin α5. One possible explanation is that integrins have much longer half-lives [over 20 hours (Liu et al., 2011)] than connexins. Therefore, the absence of 14-3-3θ only disrupts the migration of integrin α5 to cell surface, and those integrin α5 molecules already on the plasma membrane would not be affected owing to the much longer life-span of this protein. However, all of these long-lived integrin α5 molecules on the cell surface may not necessarily associate with Cx43 because of the relatively faster turnover rate of connexins. Thus, over 50% decrease of HC function is correlated with a proportionate reduction of Cx43 on the cell surface, which is likely to be associated with integrin α5.

We show that loss of HC activity in the absence of 14-3-3θ is not a consequence of the change in total Cx43 protein level but an outcome of the inefficient exit from the Golgi apparatus, resulting in reduced surface expression of Cx43 and integrin α5. 14-3-3 is a multifunctional protein known to be involved in several cellular processes. One of its emerging roles in recent years is the promotion of cell surface transport of membrane proteins by binding to the target membrane proteins and mediating their forward trafficking (Mrowiec and Schwappach, 2006; Shikano et al., 2006). 14-3-3θ binding through different motifs to several multimeric proteins was shown to correlate with expression levels of these proteins at the cell surface (O'Kelly et al., 2002; Shikano et al., 2005; Yuan et al., 2003). For example, phosphorylation-dependent binding of 14-3-3 has been demonstrated to promote cell surface expression of HIV co-receptor GPR15 by suppressing the ER recognition motif and increasing the stability of GPR15 (Okamoto and Shikano, 2011). Previous reports have suggested that 14-3-3 primarily facilitates the exit from the ER, instead of Golgi, as we observed here. One possible explanation for this

Journal of Cell Science (2014) 127, 137–146 doi:10.1242/jcs.133553

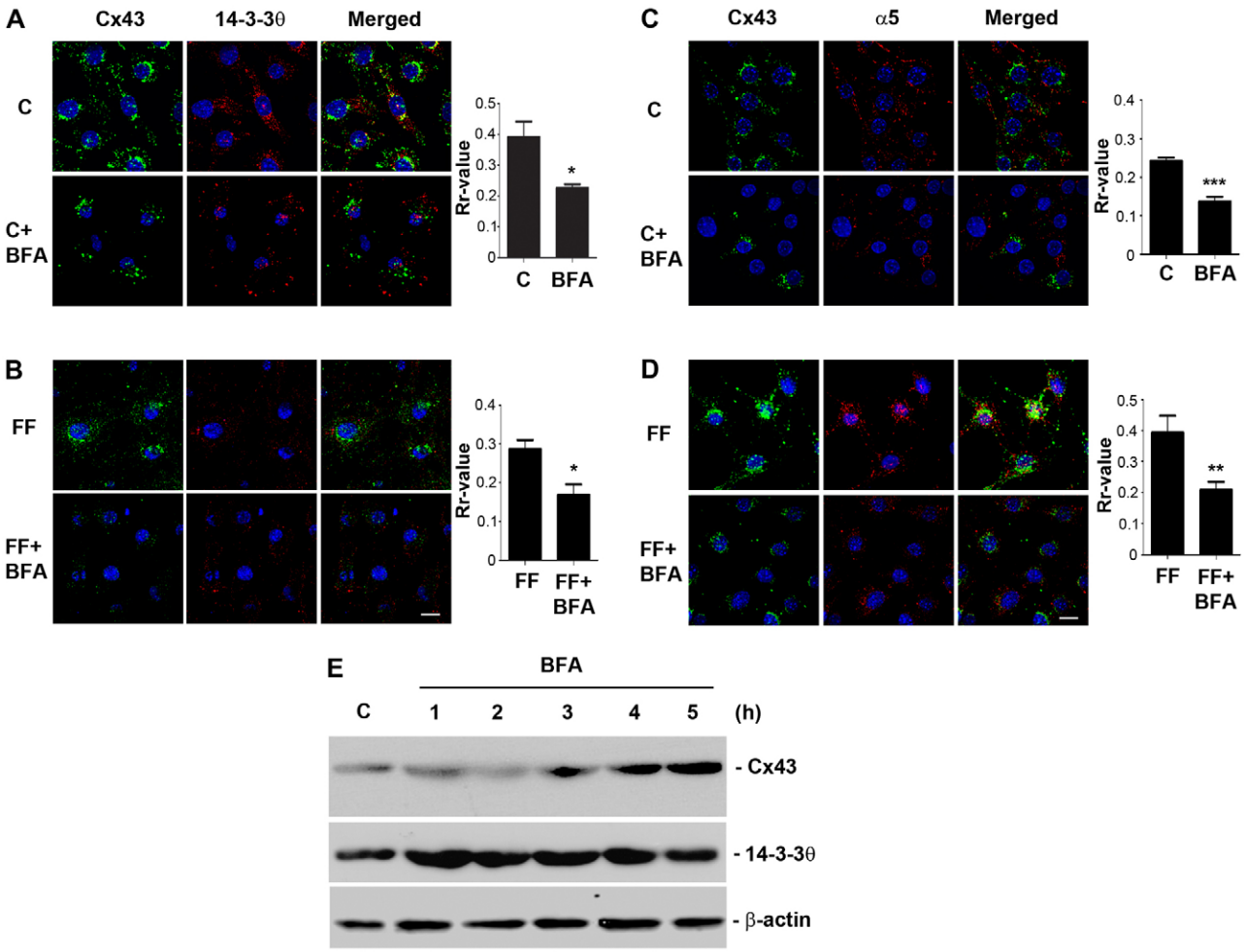

Fig. 8. Disruption of Golgi reduces the association of Cx43 and integrin α5 with 14-3-3θ. (A–D) BFA reduces the colocalization between Cx43, integrin α5 and 14-3-3θ. MLO-Y4 cells were pretreated with or without 2 μM BFA for 5 hours and were subjected to FFSS (FF; 16 dynes/cm^2; B,D) or left untreated (C; A,C) for 2 hours. Cells were fixed and dual-immunostained with antibodies against Cx43 and 14-3-3θ (A,B) or Cx43 and α5 (C,D). The colocalization is shown in the merged images. The overlap of fluorescence signals obtained were calculated using ImageJ software and a correlation coefficient (Rr) value was attained that describes the extent of overlap of the two colors. Scale bars: 10 μm. *P<0.05, **P<0.01 and ***P<0.001; n=3. (E) BFA treatment increases total Cx43 level. MLO-Y4 cells were treated with 2 μM BFA or left untreated for up to 5 hours and cell lysates were collected and immunoblotted with anti-Cx43, 14-3-3θ or β-actin antibody.

discrepancy is that unlike Cx43, the majority of oligomeric membrane proteins are assembled in the ER, instead of the Golgi. Binding of 14-3-3θ to membrane proteins containing the RXRSWTY motif on the C-terminus masks the ER localization signal in these proteins and prevents their retention in the ER (Shikano et al., 2005; Shikano et al., 2006). Cx43 is a unique membrane protein that oligomerizes in the Golgi instead of the ER (Musil and Goodenough, 1993). Indeed, a large fraction of 14-3-3θ is also reported to be localized in the Golgi (Preisinger et al., 2004). Interestingly, we observed that absence of 14-3-3θ caused the accumulation of Cx43 in the Golgi, also the site where Cx43 oligomerizes to form hexameric connexon (HC) prior to being delivered to the plasma membrane. Moreover, FFSS promoted migration of Cx43 from the Golgi to the cell surface was accompanied by increased protein levels of 14-3-3θ and a strengthened association with Cx43. The Golgi appears to be a major site for the association of 14-3-3θ with Cx43 and integrin α5. Disruption of the Golgi by BFA significantly decreases the co-localization of these proteins. Interestingly, BFA treatment decreased fluorescence signals for Cx43, but increased the total level of Cx43 protein. One possible explanation is that Cx43 is reported to be assembled in the trans-Golgi network, the collapse of the Golgi would affect the formation of the oligomerized form of Cx43. Indeed, we have observed the colocalization of Cx43 with a trans-Golgi marker, and fluid flow shear stress, which enhances the assembly of Cx43 HC, also increases the presence of Cx43 in the trans-Golgi network. It is known that fluorescence signals emitted from oligomeric proteins are much stronger than those from monomeric proteins. Cx43 retained in the ER as a result of BFA treatment exists in the form of monomers. This would explain the decreased fluorescence signals from intracellular Cx43 upon BFA treatment.

Together the results reported here show that 14-3-3θ plays an indispensable role in simultaneously transporting integrin α5 and Cx43 to the plasma membrane to form mechanosensitive HC. Opening of HC mediates the release of small bone modulators, a crucial step in the anabolic action of mechanical loading.

Journal of Cell Science (2014) 127, 137–146 doi:10.1242/jcs.133553

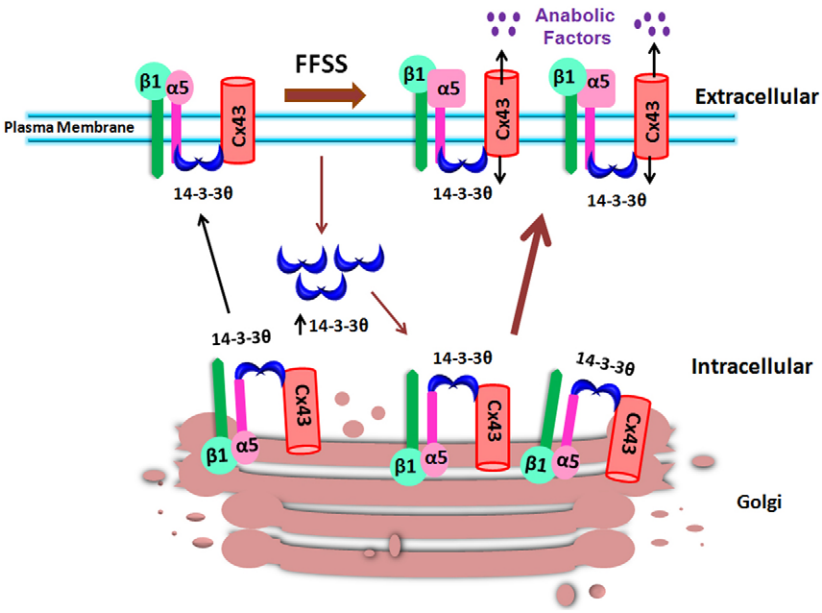

Fig. 9. Illustration of the role of 14-3-3θ in facilitating the delivery of Cx43 and integrin α5 from Golgi to the plasma membrane in response to FFSS. Under non-FFSS static conditions, there are low levels of 14-3-3θ (blue crescents) that bind to Cx43 and integrin α5β1 and move them to the plasma membrane. Under FFSS, the levels of 14-3-3θ are increased, leading to more 14-3-3θ binding to Cx43 and integrin α5β1 associated with increased movement of these two proteins out of the Golgi for assembly on the plasma membrane to form functional hemichannels. Functional hemichannels mediate the release of small autocrine and/or paracrine factors important for bone formation and remodeling under mechanical stimulation.

MATERIALS AND METHODS

Cell culture and reagents

MLO-Y4 osteocytic cells derived from murine long bones were cultured on polyester surfaces (Regal Plastics, San Antonio, TX, USA) coated with rat tail collagen type I (0.15 mg/ml; BD Biosciences, San Jose, CA, USA), and were grown in α-modified essential medium (α-MEM; Gibco-BRL, Gaithersburg, MD, USA) supplemented with 2.5% FBS and 2.5% BCS (Hyclone, Logan, UT, USA) and incubated in a 5% CO_2 incubator at 37℃ as described previously (Kato et al., 1997). S-MEM (Life Technologies, Grand Island, NY, USA) Ca^{2+} free medium, was used for the dye uptake assay. For immunostaining and dye uptake assays, cells were cultured on glass slides coated with appropriate matrices. LY and Rhodamine dextran (RD; molecular mass, 10 kDa), used for dye uptake and dye transfer assays, and BFA were obtained from Invitrogen (Life Technologies, Grand Island, NY, USA). Antibodies against integrin α5 (R&D Systems, CD49e, Minneapolis, MN, USA), monoclonal Cx43 (Santa Cruz Biotechnology, Santa Cruz, CA, USA), 14-3-3θ (Exalpha, Shirley, MA, USA) and Golgi marker 58K (Sigma-Aldrich, St Louis, MO, USA) were used for immunostaining.

Immunoprecipitation and immunoblotting

Cultured MLO-Y4 cells were collected from 150 mm tissue culture plates and lysed in PBS and spun at 10,000 ***g*** for 2 minutes to collect the cell pellet. The pellet was dissolved in RIPA buffer and then ruptured by triturating through a 26½ gauge needle 20 times. For co-immunoprecipitation, a final concentration of 0.25% Triton X-100 was used and cell lysates were incubated on ice for 30 minutes followed by a spin at 10,000 ***g*** for 10 minutes to remove the debris. RIPA buffer was added to lysates to make the final volume to 1 ml. Cell lysates were pre-cleared with 20 µl protein G beads (protein-G–Sepharose fast flow 4B; Amersham GE, Piscataway, NJ, USA) and pelleted by centrifugation at 1800 ***g*** at 4℃ for 2 minutes. Supernatants (pre-cleared lysates) were then incubated with anti-integrin α5 or anti-14-3-3θ antibodies overnight at 4℃, followed by precipitation of the complexes after incubation at 4℃ with 20 µl protein G beads or mouse IgG agarose beads. Immunoprecipitates were separated on 10% SDS-PAGE gels, and immunoblotted with affinity purified anti-Cx43 (E2; 1:300 dilution), anti-integrin α5 (1:1000) or anti-14-3-3θ (1:1000) antibody. Blots were developed by enhanced chemiluminescence (Amersham Pharmacia Biotech, Piscataway, NJ, USA).

FFSS

FFSS was created by parallel plate flow chambers separated by a gasket of defined thickness with gravity-driven fluid flow using a peristaltic pump. The thickness of the gasket determines the channel height. By adjusting the channel height and flow rate, stress levels of 16 dynes/cm^2 were generated. Controls consisted of MLO-Y4 cells in SMEM medium not subjected to fluid flow. A cell surface area of 5 cm^2 was used for dye uptake and immunofluorescence microscopy. Each test was conducted for the respective time as indicated. The circulating medium was SMEM. The entire flow system was encased within a large walk-in CO_2 incubator at 5% CO_2 and 37℃.

Immunofluorescence labeling, confocal fluorescence microscopy and colocalization analysis

The cells cultured on microscope slides coated with collagen were fixed in 4% paraformaldehyde in PBS for 20 minutes at room temperature. The cells were permeabilized with 0.25% Triton X-100 (prepared in PBS) and blocked with 3% BSA in PBS for 1 hour at room temperature (RT). The cells were then incubated for 1 hour at 4℃ with affinity-purified rabbit polyclonal antibody against the second extracellular domain of Cx43 [Cx43 (E2)], which we developed (Siller-Jackson et al., 2008) (1:300 dilution), monoclonal antibody Cx43 (1:100) or monoclonal antibody against Golgi 58K (1:50). Cells were rinsed three times with PBS and incubated for 1 hour with the appropriate secondary antibody in 3% BSA.

For surface labeling, the cells were cultured as described above, then washed in cold 1× PBS followed by incubation with polyclonal sheep anti-integrin α5 antibody against an extracellular epitope diluted in 3% PBS for 1 hour at 4℃. Cells were washed once with PBS and incubated with Cx43 antibody (1:300 diluted in 3% BSA) for 1 hour at 4℃. The cells were then washed three times with PBS and fixed in 4% PFA in PBS for 20 minutes at RT. Again, the cells were washed three times with PBS and labeled with the appropriate secondary antibodies in succession for 1 hour each at RT. Slides were mounted using Vectashield mounting medium (H-1000, Vector Laboratories, Burlingame, CA) and sealed for microscopy. Confocal fluorescence microscopy with three-dimensional z-stacking scanning was performed using a confocal laser scanning microscope (Fluoview; Olympus Optical, Tokyo, Japan). The scanning was conducted at a thickness of 0.5 µm. Images were deconvoluted using iterative deconvolution software of ImageJ with a known point spread function (applied for 30 iterations of each image with a low pass filter diameter of 1.5 pixels). Brightness and contrast were adjusted off-line to improve the clarity of each image. No data were added or deleted. In order to obtain the Pearson correlation number, as an index of colocalization, the JACoP plugin of ImageJ was used.

Scrape-loading dye transfer assay

MLO-Y4 cells were grown to ~75–85% confluency. The 'scrape-loading' dye transfer assay was performed based on the modified procedure described by El-Fouly and co-workers (El-Fouly et al., 1987). Cells were scratched in the presence of LY and RD. Cells were washed three times with HBSS plus 1% BSA. Then 1% LY and 1% RD dissolved in PBS were applied to the cells, which were subsequently scraped gently with a 26½-gauge needle. After incubation for 5 minutes, cells were washed with HBSS three times, then with PBS twice, and finally fixed in fresh 2% paraformaldehyde (from 16% stock) for 20 minutes. The dye transfer results were examined using a fluorescence microscope (Zeiss Axioscope, Zeiss, Jena, Germany), in which LY could be detected using the filter set for fluorescein, and RD using the filter set for Rhodamine. To reach statistical significance, more than 500 cells receiving RD were counted for each assay.

Dye uptake assay and inhibition experiments

MLO-Y4 cells were cultured at a density at which the majority of the cells were not physically in contact with one another. S-MEM, a Ca^{2+}-free medium, was used for the FF experiments at a flow rate of 16 dynes/cm^2 for 10 minutes. Control cells (not subjected to FF) were washed three times with S-MEM. After FF, cells were incubated for dye uptake analysis with a mixture of 0.2% LY (molecular mass ~547 Da) and 0.2% RD (~10 kDa) for 5 minutes. RD was used as a negative control. Cells were then fixed using 2% PFA for 20 minutes and washed once with PBS before mounting the slides for microscopy. Similar fields were observed under the fluorescence microscope. Dye uptake was determined as the ratio of fluorescent cells to total cells per image. Results are expressed as normalized dye uptake (designated as 1) over the respective un-stimulated control group.

14-3-3 siRNA and BFA treatment

MLO-Y4 cells were trypsinized and resuspended in antibiotic-free OPTI medium (Invitrogen, Carlsbad, CA, USA). Cells were transiently transfected as suspensions on collagen-coated slides for 48 hours with 30, 60 or 75 nM 14-3-3θ siRNA or 60 nM scrambled siRNA commercially produced by Ambion (Austin, TX, USA), using a siRNA transfection kit (Ambion). Three hours after the transfection, the medium was removed and replaced with fresh medium without antibiotics. Cells were lysed to isolate protein which was subjected to SDS-PAGE followed by immunoblotting with 14-3-3θ, Cx43, integrin α5 and GAPDH antibodies. The slides with siRNA-transfected cells were subjected to FF for 10 minutes, incubated with LY and RD, and dye uptake was examined. For the surface biotinylation assay, the cells were incubated with biotin and lysed, and equal amounts of total protein of control and siRNA-treated samples were applied to avidin-conjugated beads. The biotin-labeled samples were purified after binding to avidin-conjugated beads and separated using SDS-PAGE (Cherian et al., 2005). For BFA treatment, MLO-Y4 cells were pre-treated with 2 µM BFA for up to 5 hours and were subjected to FF for 10 minutes. Fixed cells were dual-immunolabeled with Cx43 and 14-3-3θ or Cx43 and integrin α5 antibodies, followed by the respective fluorescence-labeled secondary antibodies. Cell lysates were subjected to immunoblotting with Cx43, 14-3-3θ or β-actin antibody.

Statistical analysis

All the data were analyzed using GraphPad Prism 5.04 software (GraphPad). One-way ANOVA and Student–Newman–Keul's test were used for more than two groups, and a paired Student's *t*-test was used for comparison between two groups. Unless otherwise specified in the figure legends, the data are presented as the means ± s.e.m. of at least three determinations. Asterisks indicate the degree of significant differences compared with the controls ($*P<0.05$, $**P<0.01$, $***P<0.001$).

Acknowledgements

We thank Dr Gregg Field for generation of biotinylated integrin α5 peptide, Dr Haian Fu at the School of Medicine, Emory University for kindly providing the His-tagged 14-3-3θ construct, Tommy Nguyen for technical assistance and the people in Dr Jiang's laboratory for critical reading of the manuscript and their valuable comments.

Competing interests

The authors declare no competing interests.

Author contributions

N.B., M.A.R., S.B., J.X.J. planned the project; N.B., M.A.R., S.B. performed experiments; N.B., M.A.R., S.B. and J.X.J. analyzed the data and prepared figures; N.B., M.A.R. and J.X.J. wrote the paper.

Funding

The work was supported by the National Institutes of Health [grant numbers AR46798 to J.X.J., EY012085 to J.X.J.]; and the Welch Foundation [grant number AQ-1507 to J.X.J]. Deposited in PMC for release after 12 months.

Supplementary material

Supplementary material available online at
http://jcs.biologists.org/lookup/suppl/doi:10.1242/jcs.133553/-/DC1

References

Batra, N., Burra, S., Siller-Jackson, A. J., Gu, S., Xia, X., Weber, G. F., DeSimone, D., Bonewald, L. F., Lafer, E. M., Sprague, E. et al. (2012a). Mechanical stress-activated integrin α5β1 induces opening of connexin 43 hemichannels. *Proc. Natl. Acad. Sci. USA* **109**, 3359-3364.

Batra, N., Kar, R. and Jiang, J. X. (2012b). Gap junctions and hemichannels in signal transmission, function and development of bone. *Biochim. Biophys. Acta* **1818**, 1909-1918.

Chanson, M., Kotsias, B. A., Peracchia, C. and O'Grady, S. M. (2007). Interactions of connexins with other membrane channels and transporters. *Prog. Biophys. Mol. Biol.* **94**, 233-244.

Cherian, P. P., Siller-Jackson, A. J., Gu, S., Wang, X., Bonewald, L. F., Sprague, E. and Jiang, J. X. (2005). Mechanical strain opens connexin 43 hemichannels in osteocytes: a novel mechanism for the release of prostaglandin. *Mol. Biol. Cell* **16**, 3100-3106.

Civitelli, R. (2008). Cell-cell communication in the osteoblast/osteocyte lineage. *Arch. Biochem. Biophys.* **473**, 188-192.

Deakin, N. O., Bass, M. D., Warwood, S., Schoelermann, J., Mostafavi-Pour, Z., Knight, D., Ballestrem, C. and Humphries, M. J. (2009). An integrin-alpha4-14-3-3zeta-paxillin ternary complex mediates localised Cdc42 activity and accelerates cell migration. *J. Cell Sci.* **122**, 1654-1664.

el-Fouly, M. H., Trosko, J. E. and Chang, C. C. (1987). Scrape-loading and dye transfer. A rapid and simple technique to study gap junctional intercellular communication. *Exp. Cell Res.* **168**, 422-430.

Fritton, S. P. and Weinbaum, S. (2009). Fluid and solute transport in bone: flow-induced mechanotransduction. *Annu. Rev. Fluid Mech.* **41**, 347-374.

Gardino, A. K., Smerdon, S. J. and Yaffe, M. B. (2006). Structural determinants of 14-3-3 binding specificities and regulation of subcellular localization of 14-3-3-ligand complexes: a comparison of the X-ray crystal structures of all human 14-3-3 isoforms. *Semin. Cancer Biol.* **16**, 173-182.

Genetos, D. C., Kephart, C. J., Zhang, Y., Yellowley, C. E. and Donahue, H. J. (2007). Oscillating fluid flow activation of gap junction hemichannels induces ATP release from MLO-Y4 osteocytes. *J. Cell. Physiol.* **212**, 207-214.

Goodenough, D. A. and Paul, D. L. (2003). Beyond the gap: functions of unpaired connexon channels. *Nat. Rev. Mol. Cell Biol.* **4**, 285-295.

Han, D. C., Rodriguez, L. G. and Guan, J. L. (2001). Identification of a novel interaction between integrin beta1 and 14-3-3beta. *Oncogene* **20**, 346-357.

Hervé, J. C., Bourmeyster, N., Sarrouilhe, D. and Duffy, H. S. (2007). Gap junctional complexes: from partners to functions. *Prog. Biophys. Mol. Biol.* **94**, 29-65.

Hughes-Fulford, M. (2004). Signal transduction and mechanical stress. *Sci. STKE* **2004**, RE12.

Jacobs, C. R., Temiyasathit, S. and Castillo, A. B. (2010). Osteocyte mechanobiology and pericellular mechanics. *Annu. Rev. Biomed. Eng.* **12**, 369-400.

Kato, Y., Windle, J. J., Koop, B. A., Mundy, G. R. and Bonewald, L. F. (1997). Establishment of an osteocyte-like cell line, MLO-Y4. *J. Bone Miner. Res.* **12**, 2014-2023.

Liu, D., Bienkowska, J., Petosa, C., Collier, R. J., Fu, H. and Liddington, R. (1995). Crystal structure of the zeta isoform of the 14-3-3 protein. *Nature* **376**, 191-194.

Liu, J., He, X., Qi, Y., Tian, X., Monkley, S. J., Critchley, D. R., Corbett, S. A., Lowry, S. F., Graham, A. M. and Li, S. (2011). Talin1 regulates integrin turnover to promote embryonic epithelial morphogenesis. *Mol. Cell. Biol.* **31**, 3366-3377.

Mrowiec, T. and Schwappach, B. (2006). 14-3-3 proteins in membrane protein transport. *Biol. Chem.* **387**, 1227-1236.

Musil, L. S. and Goodenough, D. A. (1993). Multisubunit assembly of an integral plasma membrane channel protein, gap junction connexin43, occurs after exit from the ER. *Cell* **74**, 1065-1077.

Muslin, A. J., Tanner, J. W., Allen, P. M. and Shaw, A. S. (1996). Interaction of 14-3-3 with signaling proteins is mediated by the recognition of phosphoserine. *Cell* **84**, 889-897.

Nufer, O. and Hauri, H. P. (2003). ER export: call 14-3-3. *Curr. Biol.* **13**, R391-R393.

Nurmi, S. M., Gahmberg, C. G. and Fagerholm, S. C. (2006). 14-3-3 proteins bind both filamin and alphaLbeta2 integrin in activated T cells. *Ann. N. Y. Acad. Sci.* **1090**, 318-325.
O'Kelly, I., Butler, M. H., Zilberberg, N. and Goldstein, S. A. (2002). Forward transport. 14-3-3 binding overcomes retention in endoplasmic reticulum by dibasic signals. *Cell* **111**, 577-588.
Okamoto, Y. and Shikano, S. (2011). Phosphorylation-dependent C-terminal binding of 14-3-3 proteins promotes cell surface expression of HIV co-receptor GPR15. *J. Biol. Chem.* **286**, 7171-7181.
Orr, A. W., Helmke, B. P., Blackman, B. R. and Schwartz, M. A. (2006). Mechanisms of mechanotransduction. *Dev. Cell* **10**, 11-20.
Park, D. J., Freitas, T. A., Wallick, C. J., Guyette, C. V. and Warn-Cramer, B. J. (2006). Molecular dynamics and in vitro analysis of Connexin43: A new 14-3-3 mode-1 interacting protein. *Protein Sci.* **15**, 2344-2355.
Preisinger, C., Short, B., De Corte, V., Bruyneel, E., Haas, A., Kopajtich, R., Gettemans, J. and Barr, F. A. (2004). YSK1 is activated by the Golgi matrix protein GM130 and plays a role in cell migration through its substrate 14-3-3zeta. *J. Cell Biol.* **164**, 1009-1020.
Shikano, S., Coblitz, B., Sun, H. and Li, M. (2005). Genetic isolation of transport signals directing cell surface expression. *Nat. Cell Biol.* **7**, 985-992.
Shikano, S., Coblitz, B., Wu, M. and Li, M. (2006). 14-3-3 proteins: regulation of endoplasmic reticulum localization and surface expression of membrane proteins. *Trends Cell Biol.* **16**, 370-375.
Siller-Jackson, A. J., Burra, S., Gu, S., Xia, X., Bonewald, L. F., Sprague, E. and Jiang, J. X. (2008). Adaptation of connexin 43-hemichannel prostaglandin release to mechanical loading. *J. Biol. Chem.* **283**, 26374-26382.
Silver, F. H. and Siperko, L. M. (2003). Mechanosensing and mechanochemical transduction: how is mechanical energy sensed and converted into chemical energy in an extracellular matrix? *Crit. Rev. Biomed. Eng.* **31**, 255-331.
Xiao, B., Smerdon, S. J., Jones, D. H., Dodson, G. G., Soneji, Y., Aitken, A. and Gamblin, S. J. (1995). Structure of a 14-3-3 protein and implications for coordination of multiple signalling pathways. *Nature* **376**, 188-191.
Yaffe, M. B. (2002). How do 14-3-3 proteins work? – Gatekeeper phosphorylation and the molecular anvil hypothesis. *FEBS Lett.* **513**, 53-57.
Yaffe, M. B., Rittinger, K., Volinia, S., Caron, P. R., Aitken, A., Leffers, H., Gamblin, S. J., Smerdon, S. J. and Cantley, L. C. (1997). The structural basis for 14-3-3:phosphopeptide binding specificity. *Cell* **91**, 961-971.
Yuan, H., Michelsen, K. and Schwappach, B. (2003). 14-3-3 dimers probe the assembly status of multimeric membrane proteins. *Curr. Biol.* **13**, 638-646.